Title	An interstitial fluid transdermal extraction system for continuous glucose monitoring
Author(s)	Yu, H; Li, D; Roberts, RC; Xu, K; Tien, NC
Citation	Journal Of Microelectromechanical Systems, 2012, v. 21 n. 4, p. 917-925
Issued Date	2012
URL	http://hdl.handle.net/10722/175546
Rights	IEEE Journal of Microelectromechanical Systems. Copyright © IEEE

An Interstitial Fluid Transdermal Extraction System for Continuous Glucose Monitoring

Haixia Yu, Dachao Li, Robert C. Roberts, Kexin Xu, and Norman C. Tien

***Abstract*—A novel microfluidic system which is fabricated with five polydimethylsiloxane layers for interstitial fluid (ISF) extraction, collection, and measurement toward the application of continuous and real-time glucose monitoring is presented in this paper. The system consists of a micro vacuum generator for ISF transdermal extraction and fluid manipulation, micro chambers for the collection of ISF, micro pneumatic valves for fluid management, and a micro flow sensor for ISF volume measurement. Sequentially controlled by the pneumatic valves, the ISF extraction, collection, and volumetric measurement functions of the system were demonstrated using the stable vacuum generated by the integrated vacuum generator. Through low-frequency ultrasound pretreated full-thickness pig skin, the normal saline solution with different glucose concentrations was transdermally extracted, collected, and measured. The absolute error in the volume measurement of the transdermally extracted "ISF analog" was less than 0.05 μL. The microfluidic system makes it possible to realize the clinical application of continuous glucose monitoring based on ISF transdermal extraction technology. [2011-0329]**

***Index Terms*—Continuous glucose monitoring, interstitial fluid (ISF), microfluidic system, transdermal extraction.**

I. Introduction

DIABETES IS a pandemic forcing millions of people to measure their blood glucose levels daily. Conventional self-testing methods require a drop of blood in the range of 0.3–10.0 μL[1] for each glucose measurement, a painful and inconvenient procedure with poor patient compliance. In addition, effective diabetes control requires frequent and accurate glucose monitoring. Consequently, there has been, and continues to be, considerable investments in the development of continuous glucose monitoring technologies [2]–[7]. A variety of techniques are being examined, including optical sensors [8], the physical implantation of devices to measure glucose directly in a local subcutaneous environment, and the minimally invasive glucose monitoring methods which test the glucose level using transdermally extracted interstitial fluid (ISF) [9]. Although monitoring glucose levels using optical techniques is truly noninvasive, an affordable, efficient, and portable optical system is not in the immediate future. Subcutaneously implanted glucose sensors are commercially available from DexCom [10], Medtronic [11], and Abbott Laboratories [12]. However, the implantation of these sensors is invasive, and these sensors require frequent calibration to mitigate instabilities over time, making long-term operation difficult [13].

Contrary to the previously mentioned techniques, transdermal extraction of ISF offers an attractive method of minimally invasive blood glucose monitoring. In this method, a sample of ISF is transdermally extracted and subsequently analyzed for glucose concentration. Good correlation between the glucose concentration of the extracted ISF and the blood glucose concentration was reported [3], [14]. However, this approach is limited by the low permeability of the human skin to glucose due to the outermost stratum corneum (SC) layer. A variety of approaches have been suggested to enhance the transdermal transport of molecules [15]. These include the use of chemicals to modify the skin structure [16], the application of electric fields [17], and the application of ultrasound [18]. After the skin permeability is increased by ultrasound pretreatment, the elevated skin permeability can persist for at least 42 h under occlusion [19], and ISF can be transdermally extracted with higher fluxes as vacuum is applied to enhance the convection of ISF [3]. High fluxes of analytes are beneficial by having high detectable analyte concentrations and short collection times, by requiring a smaller skin area for sampling, and by lowering interference from background analytes (i.e., sweat) [14]. Although the transdermal ISF extraction technique using ultrasound and vacuum offers the promise of noninvasive, continuous, and real-time glucose monitoring, this technique only extracts a minute volume of ISF, which scatters on the skin surface, making it unsuitable for ISF collection and measurement by using macroscale systems. In order to collect the minute volume of ISF, a certain volume of normal saline, which is similar to the ISF, is required to mix with the transdermally extracted ISF and form a manipulable volume of fluid for easy collection. In addition, due to the variation of skin permeability with time [20], the volumes of transdermally extracted ISF will also vary. As a result, the glucose concentration of the collected fluid is not only affected by the glucose concentration of ISF, but also by the volume ratio between the transdermally extracted ISF and the normal saline solution used to help collect ISF. Therefore, it is critical to make precise ISF volume measurements in order to calculate blood glucose concentrations accurately.

In this paper, a novel integrated microfluidic system capable of automatic extraction, collection, and volumetric

Manuscript received November 8, 2011; revised February 17, 2012; accepted March 21, 2012. Date of publication April 26, 2012; date of current version July 27, 2012. This work was supported in part by the National Natural Science Foundation of China (30800239, 60938002, and 61176107), in part by the Key Projects in the Science and Technology Pillar Program of Tianjin (11ZCKFSY01500), and in part by the Innovation Foundation of Tianjin University. Subject Editor A. J. Ricco.

H. Yu, D. Li and K. Xu are with the State Key Laboratory of Precision Measuring Technology and Instruments, Tianjin University, Tianjin 300072, China (e-mail: dchli@tju.edu.cn).

R. C. Roberts and N. C. Tien are with the Department of Electrical Engineering and Computer Science, Case Western Reserve University, Cleveland, OH 44106 USA.

Color versions of one or more of the figures in this paper are available online at http://ieeexplore.ieee.org.

Digital Object Identifier 10.1109/JMEMS.2012.2192910

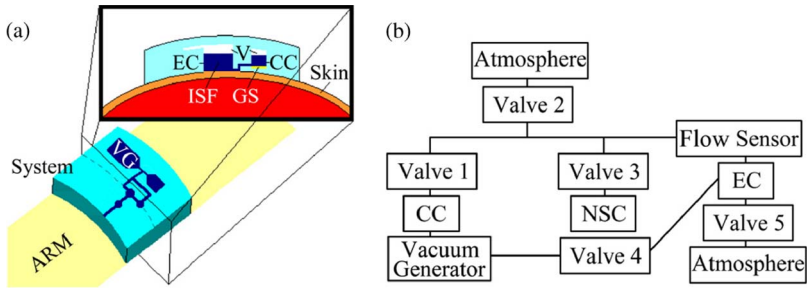

Fig. 1. Schematic view of the system. EC: Extraction Chamber, CC: Collection Chamber, V: Vacuum, GS: Glucose Sensor, VG: Vacuum Generator, NSC: Normal Saline Chamber.

TABLE I
VALVE SEQUENCING WORKFLOW

Step	Valve Status: C–Closed, O–Open					Function
	1	2	3	4	5	
I	C	C	C	C	C	Generate vacuum.
II	C	C	O	O	C	Extract normal saline from NSC to EC, test resistance between electrodes E4 of flow sensor.
III	C	O	C	O	C	Input defined volume of normal saline.
IV	C	C	C	O	C	Extract ISF.
V	O	C	C	C	O	Collect and test the volume of the sample.
VI	C	C	C	C	C	Finish.

measurement of the ISF is developed. This device overcomes the fluid handling hurdles that are crucial for a low-cost and portable ISF-based glucose monitoring system.

II. STRUCTURE DESIGN

A. System Overview

The schematic view of a microfluidic continuous glucose monitoring device which can be worn similarly to a watch is shown in Fig. 1(a). The device monitors blood glucose level based on the measurement of transdermally extracted ISF. It consists of a microfluidic system for ISF transdermal extraction, collection, and volumetric measurement, which is present in this paper, and a micro glucose sensor which is under development. As shown in Fig. 1(b), the microfluidic system is composed of a vacuum generator, pneumatic valves, a flow sensor, fluid chambers, and interconnecting microfluidic channels.

The vacuum generator is used to provide the driving force for both ISF extraction and fluid manipulation during normal saline injection and ISF collection processes. The pneumatic valves are computer programmed to sequentially control the ISF extraction, collection, and volumetric measurement processes (refer to Table I). The flow sensor, which monitors the electrolytic fluid flowing between the chambers, is integrated into the microfluidic channel to enable accurate volumetric measurement of the extracted ISF. Finally, the fluid chambers are used for the introduction of normal saline solution and the extraction and collection of ISF.

During the ISF extraction, collection, and volumetric measurement processes, the vacuum generator first provides a stable vacuum to prepare for the subsequent actions. Next, a defined volume of normal saline, which is stored in the normal saline chamber, is injected into the extraction chamber to help collect the scattered ISF. During actual operation, the extraction chamber is sealed to the skin [as shown in Fig. 1(a)], enabling the system to harvest ISF. Vacuum is then applied to the extraction chamber for ISF extraction, and as the ISF is retrieved, it mixes with the normal saline to form a manipulable volume of fluid. After extraction, the fluid volume is measured as it transfers from the extraction chamber to the collection chamber where a glucose sensor will ultimately reside. Calculating the volume difference between the initial defined volume and the post extraction measured volume yields the amount of extracted ISF, which is the key to obtaining accurate glucose monitoring.

B. Structure Design of the Micro Vacuum Generator

In order to establish a miniaturized and integrated system, a compact vacuum generator is required for this application. The Venturi tube, which is simple in design and can be fabricated on a single mask layer, is selected as the core component of the vacuum generator for the application of transdermal ISF extraction and fluid manipulation. The simple Venturi tube is designed using the following equation, which originates from Bernoulli's equation:

$$P_1 - P_2 = \rho\left(v_2^2 - v_1^2\right)/2 = \rho v_1^2\left(A_1^2/A_2^2 - 1\right)/2 \quad (1)$$

where P_1 is the input pressure, P_2 is the output vacuum, ρ is density, v_1 is the velocity of the input fluid, v_2 is the velocity of the fluid in the vena contracta section, and A_1 and A_2 are channel areas of the input section and the vena contracta section, respectively. By forcing the gas through the convergent and the vena contracta sections, the gas velocity increases and results in a pressure drop that is greatest just before the divergent section toward the outlet. Under the correct conditions, pressures less than the ambient (vacuum) can be generated, which are used for ISF extraction and fluid manipulation. The structure of the vacuum generator in this system was optimized to be suitable for microfluidics. A dimensioned diagram of the optimized geometry for this work is shown in Fig. 2. The width and height of the vena contracta section are both 230 μm, and the ratio of the width of the input section to that of the vena contracta section is 37 : 1.

C. Structure Design of the Micro Pneumatic Valve

A micro pneumatic valve is designed to manage the ISF extraction, collection, and volumetric measurement processes

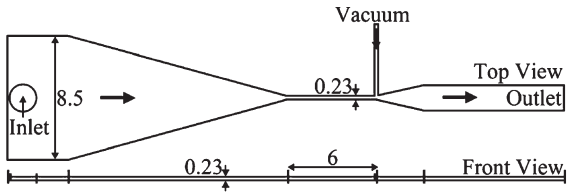

Fig. 2. Dimensioned drawing of vacuum generator. Units are shown in mm.

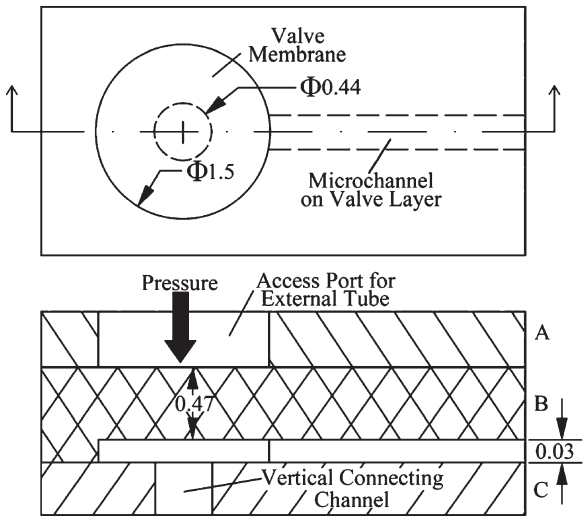

Fig. 3. Structure of pneumatic valve (Unit: mm). A: vacuum generator layer, B: valve layer, C: flow sensor layer.

under computer control. The pneumatic valve with a simple structure is easy to control and responds rapidly.

The structure of the pneumatic valve fabricated with polydimethylsiloxane (PDMS) is shown in Fig. 3. When an external pressure is applied on the surface of the valve membrane, the membrane will deflect to the flow sensor layer and connect to the vertical connecting channel. As a result, the connection between the microfluidic channel on the valve layer and the vertical connecting channel will be blocked, causing the valve to close. When the external pressure is restored to atmospheric pressure, the valve will reopen.

When the circular PDMS membrane of radius a carries a pressure p that is uniformly distributed over the entire surface of the valve membrane, the deflection of the membrane at a distance r from the center of the membrane is determined by the equation

$$w = \frac{p(a^2 - r^2)^2}{64D} \tag{2}$$

where the flexural rigidity of the membrane D is determined by the equation

$$D = \frac{Eh^3}{12(1 - \upsilon^2)} \tag{3}$$

where E is Young's modulus, h is thickness of the membrane, and ν is Poisson's ratio. According to (2) and (3), the pressure

TABLE II
PARAMETERS OF THE VALVE MEMBRANE

E (kPa)	v	h (μm)	a (μm)	r (μm)	w (μm)
750	0.5	470	750	220	30

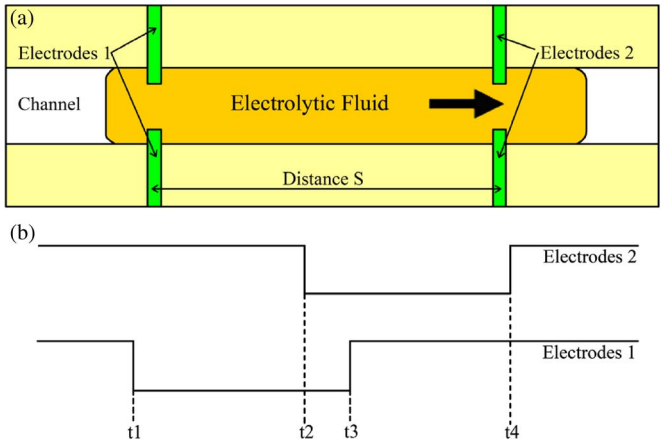

Fig. 4. (a) Schematic of the flow sensor with two pairs of electrodes for a situation corresponding to the time period between t2 and t3. (b) Timing diagram of the electrodes resistance.

that will cause the pneumatic valve to close is determined by the equation

$$p = \frac{64Dw}{(a^2 - r^2)^2} = \frac{16}{3} \cdot \frac{Eh^3 w}{(1 - \upsilon^2)(a^2 - r^2)^2}. \tag{4}$$

Based on the properties of PDMS and the dimensions of the pneumatic valve, the parameters of the valve membrane are presented in Table II. Utilizing these parameters and (4), the pressure needed to close the valve was calculated and determined to be 62.85 kPa (relative pressure).

D. Structure Design of the Micro Flow Sensor

The viability of this system hinges on the ability to accurately measure the amount of normal saline solution and ISF in order to provide essential information for accurate continuous glucose monitoring. Utilizing the conductivity of the electrolytic fluid (e.g., normal saline, ISF) in our application, a flow sensor that is simple in operation and readily integrated has been obtained. The flow sensor comprises of electrode pairs located in a microfluidic channel of a fixed dimension. Each pair of electrodes is separated by a small gap inside the channel such that the electrolytic fluid flowing through the channel will bridge the gap, and the resistance between the electrodes will decrease sharply. During operation of the system, the resistance of each electrode pair and the timing of any resistance change are monitored. In addition, the duration of the changes in the electrode pair resistance and the dimensions of the microfluidic channel are used to calculate the volume of the electrolytic fluid.

The stable vacuum generated from the vacuum generator uniformly accelerates the electrolytic fluid in the uniform microfluidic channel in the ISF transdermal extraction, collection, and volumetric measurement system. The schematic of a flow sensor with two pairs of electrodes is shown in Fig. 4(a), and

the corresponding timing diagram of the electrodes' resistance is shown in Fig. 4(b). The head of the electrolytic fluid section passes Electrodes 1 (E1) at time t_1, and its velocity and acceleration are defined as v_1 and a, respectively. When the fluid section flows through the channel at time t_2, t_3, and t_4, its velocity is $v_2 = v_1 + a(t_2 - t_1)$, $v_3 = v_1 + a(t_3 - t_1)$, and $v_4 = v_1 + a(t_4 - t_1)$, respectively.

Therefore, the distance between the two pairs of electrodes S and the length of the liquid section L can be expressed as follows:

$$\begin{aligned} S &= [v_1 + v_1 + a(t_2 - t_1)]\,(t_2 - t_1)/2 \\ &= [v_1 + a(t_3 - t_1) + v_1 + a(t_4 - t_1)]\,(t_4 - t_3)/2 \quad (5) \\ L &= [v_1 + v_1 + a(t_3 - t_1)]\,(t_3 - t_1)/2. \quad (6) \end{aligned}$$

From (5), v_1 and a are obtained as follows:

$$v_1 = \frac{S\left[t_4^2 - t_3^2 - t_2^2 - t_1^2 - 2t_1(t_4 - t_3 - t_2)\right]}{(t_4 - t_3)(t_2 - t_1)(t_4 + t_3 - t_2 - t_1)} \quad (7)$$

$$a = \frac{2S(-t_4 + t_3 + t_2 - t_1)}{(t_4 - t_3)(t_2 - t_1)(t_4 + t_3 - t_2 - t_1)}. \quad (8)$$

Insert v_1 and a into (6) and L is obtained

$$L = \frac{S(t_3 - t_1)(t_4 - t_2)(t_4 - t_3 + t_2 - t_1)}{(t_4 - t_3)(t_2 - t_1)(t_4 + t_3 - t_2 - t_1)}. \quad (9)$$

The exceptional case for uniformly accelerated motion is uniform motion. As such, when the duration of the electrolytic fluid section flowing through the flow sensor is very short, the uniformly accelerated motion can be simplified to uniform motion. For uniform motion, the constant velocity is v_1 and the acceleration a equals zero, that is to say $t_4 - t_3 = t_2 - t_1$. Therefore,

$$L = \frac{S(t_3 - t_1)}{(t_2 - t_1)}. \quad (10)$$

Since the geometry of the flow channel is known, the volume of fluid can then be calculated as follows:

$$V = LWH \quad (11)$$

where W and H are the width and height of the channel, respectively.

According to the volumetric measurement principle of the flow sensor with two pairs of electrodes, a flow sensor with four pairs of electrodes is designed in the system to satisfy the requirements for accurately measuring the ISF volume. In order to decrease the length of the flow sensor, a curved microfluidic channel is used instead of the straight microfluidic channel.

III. Fabrication Process

In order to prove the viability of this concept, the system was fabricated from five PDMS layers (shown in Fig. 5): the vacuum generator layer, the valve layer, the flow sensor layer, the electrodes layer, and the bottom layer. Except for the electrodes layer, every layer was fabricated using standard SU-8 micromolding techniques. The electrodes on the surface of the electrodes layer were fabricated using conductive PDMS similar to the method utilized by Niu *et al.* [21]. However, a laser cut Kapton tape patterning process had been developed that substituted the micromold fabrication with a photo resist.

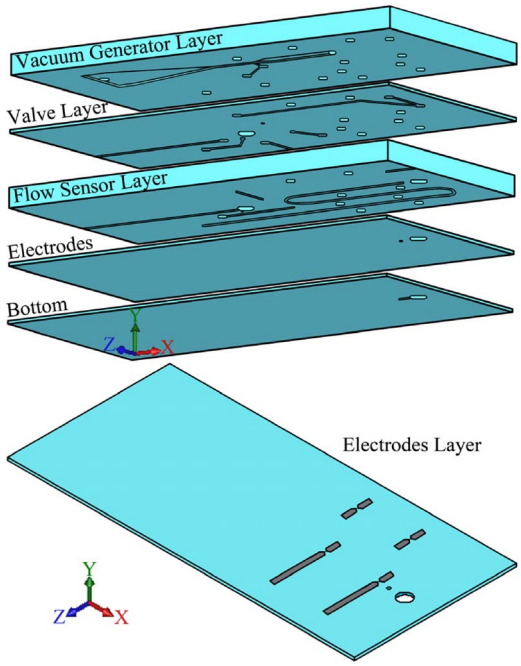

Fig. 5. Schematic view of the system with five PDMS layers.

A. Processes for Micromolding the PDMS Layers

1) SU-8 100 (MicroChem) was spun on a bare 100-mm silicon wafer. The SU-8 was subsequently lithographically patterned to form molds of the desired geometry.
2) PDMS (Sylgard 184, Dow Corning) was mixed in a 10 : 1 ratio of PDMS base with the curing agent. After 45 min of degassing in the vacuum jar, the PDMS was poured onto SU-8 molds.
3) The PDMS layers cured at 80 °C for one hour were peeled from the molds.

B. Processes for Fabricating the Electrodes Layer

1) Kapton tape adhering to the aluminum plate was cut by a laser (VersaLASER VLS 3.50), and the electrode parts were peeled from the aluminum plate.
2) Kapton tape left on the aluminum plate was cleaned in an ultrasonic bath and moved to a 100-mm glass wafer.
3) Ag microparticles were mixed with PDMS in a 4 : 1 weight ratio to form conductive PDMS.
4) After the conductive PDMS was plastered on the Kapton tape, the Kapton tape was peeled carefully from the glass wafer, and the conductive PDMS electrodes were left on the surface of the glass wafer.
5) The conductive PDMS electrodes were cured at 80 °C for one hour, and the PDMS was poured onto the surface of the glass wafer.

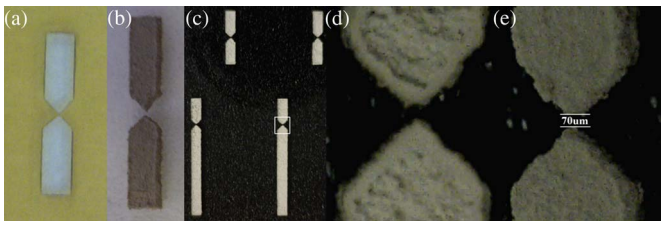

Fig. 6. (a) Laser cut Kapton tape adhering to a glass wafer. (b) Conductive PDMS electrodes on a glass wafer. (c) Photograph of PDMS sheet with electrodes. (d) and (e) are enlarged views of the highlighted part in (c) taken from electrode side and PDMS side, respectively.

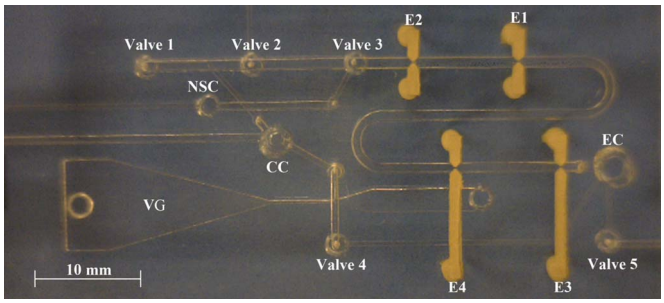

Fig. 7. Photograph of the system. NSC: Normal Saline Chamber, EC: Extraction Chamber, CC: Collection Chamber, VG: Vacuum Generator. E1, E2, E3, and E4 are four pairs of electrodes.

6) The PDMS layer cured at 80°C for one hour was peeled from the glass wafer to obtain the electrodes layer.

C. Processes for Integrating the Five PDMS Layers

1) The access ports for the external tubes and the air vent of the vacuum generator were punched in the vacuum generator layer.
2) The vertical interconnecting channels between the different layers and the chambers were drilled and punched in the other four layers.
3) The five layers of PDMS were aligned and bonded together using oxygen plasma (900 mTorr O_2, 25 W, 25 s).

D. Fabrication Results

Using the illustrated fabrication process, an ISF transdermal extraction, collection, and volumetric measurement system was obtained. Photographs of the electrodes and the completed system are shown in Figs. 6 and 7, respectively.

IV. Results and Discussions

A complete system test was performed to verify the functionality of the system. The vacuum for ISF extraction and fluid manipulation, the pressure required to close the pneumatic valve, and the ISF volume measurement function of the system were tested.

A. Test Results of the Vacuum Generator

The schematic diagram of the experimental setup for the vacuum generator output vacuum measurements is shown in Fig. 8. A N_2 gas cylinder provided the external pressure that was regulated and applied to the vacuum generator through the pressure inlet. This external pressure was measured using a pressure sensor (40PC100G2A, Honeywell Sensing and Control). A vacuum pressure sensor (40PC015V2A, Honeywell Sensing and Control) was connected to the microfluidic channel on the left side of the collection chamber. Five nylon tubes (only one line of connection is shown in Fig. 8) fixed on the top of the pneumatic valve membrane were connected to five solenoid valves (M125 AE1 LW 24 VDC, Humphrey). The state of the pneumatic valve was determined by the pressure on the top of its membrane. After regulation, the external pressure generated from the N_2 gas cylinder was applied to the solenoid valves. When the solenoid valve opened, the external pressure was applied to the pneumatic valve of the system and would cause the valve to close. Otherwise, the external pressure was obstructed and the top of pneumatic valve membrane was exposed to the atmosphere, which allowed the pneumatic valve to remain open and for fluid to flow through the corresponding microfluidic channel. A data acquisition interface (NI USB-M6251) was used to sample and record the input pressure and the output vacuum signal of the vacuum generator and to control the solenoid valve. When the five pneumatic valves were all closed, both of the vena contracta section of the vacuum generator and the vacuum pressure sensor were connected to the collection chamber. The output vacuum of the vacuum generator was measured by controlling the valve states and by regulating the input pressure.

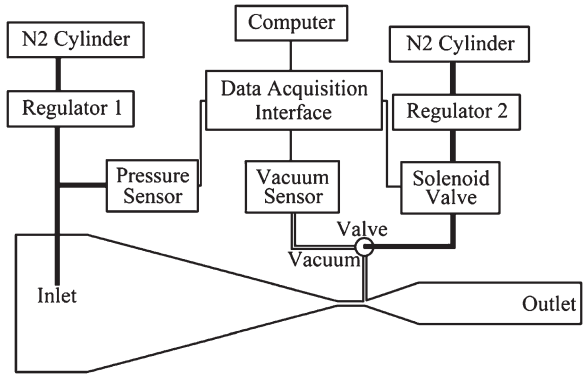

Fig. 8. Schematic diagram of experimental setup for vacuum generator output vacuum measurements.

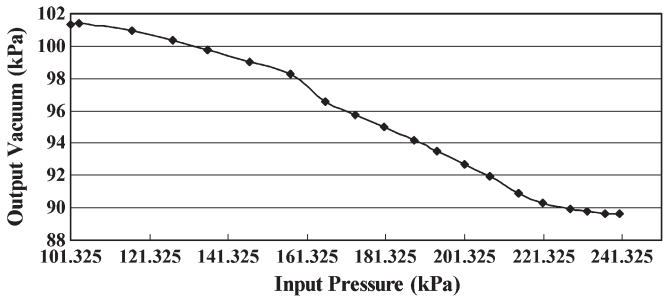

Fig. 9. Output vacuum of vacuum generator versus input pressure.

As shown in Fig. 9, a vacuum pressure of less than 91 kPa was achieved when a pressure of 220 kPa was applied. This level of vacuum is sufficient for ISF extraction and fluid manipulation in our system.

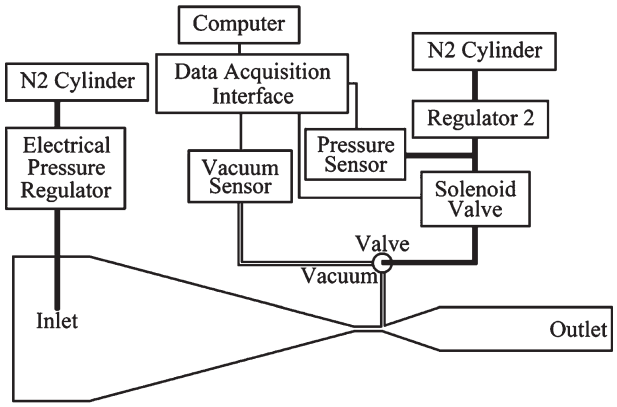

Fig. 10. Schematic diagram of experimental setup for pneumatic valve close pressure measurements.

Despite the fact that Venturi tube can provide adequate vacuum pressure and pumping speed for the application of transdermal ISF extraction and fluid manipulation, a micro pressure generator is required to be integrated into the inlet section of the Venturi tube to complete a micro vacuum generator for miniaturized system. For this purpose, a micro pressure generator using a solid chemical propellant to stably produce N_2 is under research in our lab. And it will be integrated into our next generation system.

B. Test Results of the Pneumatic Valve

To measure the pneumatic valve actuation pressure, regulator 1, which was connected to the inlet of the vacuum generator, was substituted with an electrical pressure regulator as shown in Fig. 10. The pressure sensor was used to measure the valve close pressure, and the vacuum pressure sensor was used to monitor the output vacuum flowing through the valve. The output pressure of the electrical pressure regulator fluctuated slightly around the pressure set point, resulting in a slight fluctuation of the output vacuum of the vacuum generator. Therefore, the output signal from the vacuum pressure sensor did not stop fluctuating until the pressure from regulator 2 was great enough to close the pneumatic valve. In order to overcome this, the pressure on the surface of the pneumatic valve membrane was regulated, and the vacuum and the pressure were measured and recorded when the vacuum output ceased fluctuating.

The pressure required to close each pneumatic valve was measured by varying valve actuation in a coordinated manner. For example, the pressure required to close valve 5 was measured when valves 1, 2, and 3 were closed, valve 4 was open, and the vacuum pressure sensor was connected to the microfluidic channel on the right of valve 5. The pressures required to close pneumatic valve 5 under different vacuum pressures are listed in Table III. As presented in Table III, the Valve Close Pressure is less than 160 kPa. In addition, the average of the differences between the Valve Close Pressure and the Vacuum under Valve Membrane is about 59.5 kPa, which is close to the calculated result (62.85 kPa).

TABLE III
CLOSE PRESSURES OF PNEUMATIC VALVE 5

Valve Close Pressure (kPa)	Vacuum under Valve Membrane (kPa)	Relative Close Pressure (kPa)
159.7	98.8	60.9
155.7	96.1	59.6
151.9	93.8	58.1

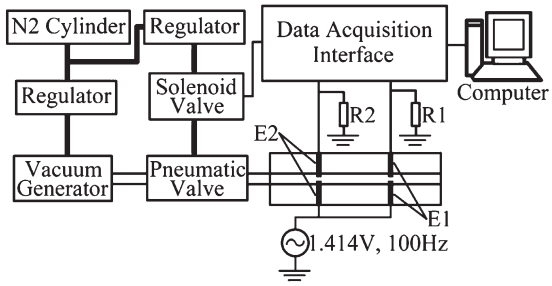

Fig. 11. Schematic diagram of experimental setup for ISF volume measurements.

C. Test Results of the Flow Sensor

The schematic diagram of the experimental setup for the flow sensor to measure the volume of ISF is shown in Fig. 11. Four 10 MΩ resistors (R1, R2, R3, and R4) and four pairs of electrodes (E1, E2, E3, and E4) were connected in series, respectively. A 1.414 V, 100 Hz AC voltage was applied to these four series circuits. In Fig. 11, the flow sensor and the experimental setup are simplified; only two pairs of electrodes and their corresponding experimental setups are shown. The voltage change across the 10 MΩ resistor represented the resistance change of the corresponding electrode pair. After signal conditioning (impedance reduction and 60 Hz noise filtering), the voltage data was inputted into the computer through a data acquisition interface. The sampling frequency was 1 kHz. Under the management of the pneumatic valves, a 95-kPa vacuum generated from the vacuum generator in the system was used for fluid manipulation during normal saline injection and sample collection processes. During the injection of normal saline, the voltage on resistor R4 was detected and used to determine the valve status in order to control the input volume of normal saline. During the collection of the sample, the voltage on the four resistors was measured, and the duration of voltage change was used to calculate the volume of the sample and the volume of ISF.

In order to test the accuracy of the integrated flow sensor for ISF volume measurement, a simulated ISF extraction was performed. Normal saline solutions with a known volume between 0 and 3 μL were used to simulate the transdermally extracted ISF and were injected into the extraction chamber with a microsyringe (701 N 10 μL, Hamilton) before the input process of 9.70 μL (this defined volume was determined by the volume of the microfluidic channel between valve 3 and electrode pair E4 and was measured by a microsyringe to inject and extract normal saline solution in the microfluidic channel) of normal saline solution. The defined volume was then transferred into the extraction chamber, mixed with the normal saline simulating the ISF, collected from the extraction

TABLE IV
FLOW SENSOR TEST RESULTS COMPARED TO MICROSYRINGE

Added Volume	Sample Volume	Tested Mean Volume	Standard Deviation	Tested Added Volume	Absolute Error
0.00	9.70	9.656	0.039	0.000	0.000
0.50	10.20	10.119	0.043	0.463	0.037
1.00	10.70	10.682	0.032	1.026	0.026
1.50	11.20	11.168	0.057	1.512	0.012
2.00	11.70	11.779	0.048	2.123	0.123
2.50	12.20	12.246	0.030	2.590	0.090
3.00	12.70	12.818	0.068	3.162	0.162

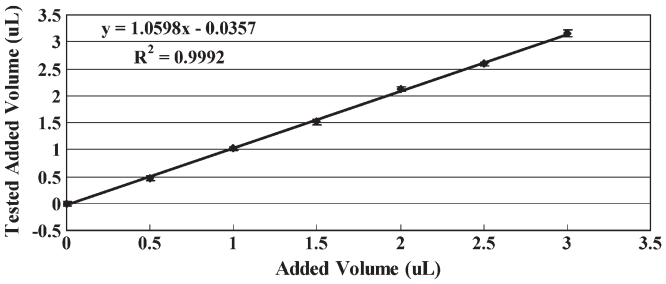

Fig. 12. Tested added volume measured by flow sensor versus Added Volume by microsyringe.

chamber to the collection chamber, and measured using the flow sensor. Six different volumes from 0 to 3 μL were tested in fixed increments of 0.5 μL to simulate varied ISF volumes. For each volume, the simulated ISF volume test was repeated 5 times.

The flow sensor test results of the simulated ISF volume measurements are presented in Table IV. The tested mean volume was the average $(n = 5)$ of the sample (mixture of the normal saline simulating the ISF and the normal saline with defined input volume) volume measured by the flow sensor. The tested added volume was calculated as the difference of the tested mean volume between the sample and the defined input normal saline. The correlation between the tested added volume and the added volume measured by the microsyringe is shown in Fig. 12. As presented in Table IV, the standard deviation for every sample is less than 0.07 μL, and the absolute error of the added volume (to simulate the transdermally extracted ISF volume) measurement is less than 0.17 μL. Specifically, when the added volume is no more than 1.50 μL, the absolute error is less than 0.04 μL. The correlation coefficient of the measurement between the tested added volume and the added volume measured by the microsyringe is $R^2 = 0.9992$, which indicates a strong relationship between the volume measured by the flow sensor and the extracted ISF volume.

D. Results of ISF Extraction Through Pig Skin

Through low-frequency ultrasound pretreated pig skin which has the same basic structure as human skin, ISF transdermal extraction, collection, and volume measurement were performed to verify the functionalities of the system.

After sacrificing the pig, the hair on the back and the abdomen were shaved with a blade, and the skin was harvested immediately. Superfluous tissues such as fat and muscle were removed carefully. Skin, with the exception of flawed pieces which had visible imperfection such as scratches and abrasion,

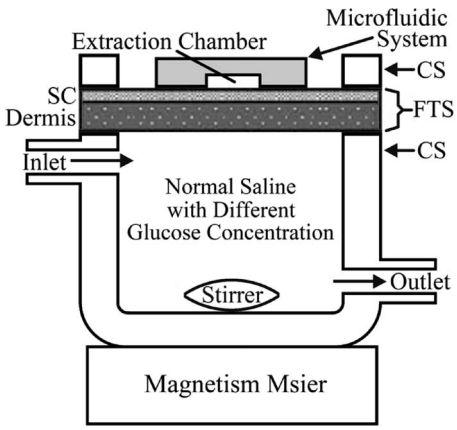

Fig. 13. Schematic diagram of the experimental setup for ISF transdermal extraction through pig skin. SC: Stratum Corneum, FTS: Full-Thickness Skin, CS: Clamping Structure.

was cut into small pieces (10 cm $\times$ 10 cm) and was stored in a -20 °C freezer for up to 4 weeks until the experiments were performed.

The schematic diagram of the experimental setup for ISF transdermal extraction through pig skin is shown in Fig. 13. Before each experiment, the skin was thawed at room temperature, pretreated by low-frequency ultrasound (SonoPrep, Sontra Medical), and mounted onto a container which was filled with normal saline solution with different glucose concentrations (1000, 1500, and 2000 mg/dL). The "ISF analog" was stirred continuously throughout the experiment. The system was held on the top of the skin with the ultrasound treated skin directly underneath the extraction chamber. A 95-kPa vacuum generated from the vacuum generator in the system was used for "ISF analog" transdermal extraction and fluid manipulation. After the vacuum pressure was connected to the extraction chamber, the skin underneath the extraction chamber swelled and bulged into the extraction chamber, thus the extraction chamber was well sealed with the skin. The duration of ISF transdermal extraction was set to be 10 min which was chosen for the final glucose monitoring goal to display and record the glucose concentration once every 10 min for one day after a single ultrasound pretreatment. Following the workflow described in Table I, the transdermally extracted "ISF analog" was at last collected into the collection chamber. During the collection procedure, the volume of the extracted "ISF analog" was measured using the integrated flow sensor. Finally, the glucose concentration of the sample in the collection chamber was tested (FreeStyle Freedom, Abbott).

The sample in the collection chamber was the mixture of the transdermally extracted "ISF analog" and the normal saline with defined input volume. The glucose concentration of the "ISF analog" C_{ISF} and the defined input volume of the normal saline V_{NS} were known, and the glucose concentration of the sample C_{S} was tested. Therefore, the volume of the transdermally extracted "ISF analog" V_{ISF} can be calculated as: $V_{\mathrm{ISF}} = V_{\mathrm{NS}} \cdot C_{\mathrm{S}}/(C_{\mathrm{ISF}} - C_{\mathrm{S}})$. The "ISF analog" volume measurement results of the integrated flow sensor were compared with the calculated results.

TABLE V
TRANSDERMALLY EXTRACTED ISF VOLUME TEST RESULTS
(DEFINED INPUT VOLUME: 8.40 μL.)

ISF Analogue Glucose Concentration (mg/dL)	Sample Glucose Concentration (mg/dL)	Calculated Volume (μL)	Measured Volume (μL)	Absolute Error (μL)
1000[1d]	246	2.738	2.720	0.019
1000[1e]	273	3.151	3.125	0.026
1000[2d]	255	2.873	2.848	0.025
1500[1a]	34	0.194	0.233	0.039
1500[1b]	71	0.416	0.387	0.028
1500[1c]	115	0.696	0.662	0.034
2000[2a]	42	0.179	0.206	0.027
2000[2b]	165	0.755	0.719	0.037
2000[2c]	422	2.245	2.290	0.045

[1a]Two pieces of pig skin were tested. The numbers "1" and "2" refer to the two pieces of skin. The letters from "a" to "e" refer to the sequence of measurement.

Under the management of the pneumatic valves and by using the 95-kPa vacuum force generated from the vacuum generator, this system was used to transdermally extract and collect the "ISF analog" through ultrasound pretreated pig skin and to measure the volume of the transdermally extracted "ISF analog." Two pieces of pig skin were tested in the experiment. The "ISF analog" volume measurement results of the flow sensor were compared with the calculated results from the tested glucose concentrations of the sample. As presented in Table V, the volumes of "ISF analog" which was transdermally extracted using a 95-kPa vacuum in 10 min are between 0 and 3.5 μL. This proves the feasibility of using the vacuum generator, which can achieve a vacuum pressure of less than 91 kPa, for ISF extraction. In addition, the absolute error of the volume measurements is less than 0.05 μL. The low absolute error values of the measurement results indicate a high accuracy of the integrated flow sensor. It proves the feasibility of using the flow sensor for ISF volume measurement.

As shown in Table V, the transdermally extracted ISF volumes increased gradually with the extraction times for both of the skin pieces. The possible reason for the volume enhancement is following. In the process of ISF transdermal extraction, the skin underneath the extraction chamber swelled under vacuum pressure. On the skin surface, the pores generated in the ultrasound pretreatment were enlarged. In addition, the in vitro skin lacks elasticity to return to its original size and shape. Therefore, the skin permeability increased gradually.

In order to develop a continuous glucose monitoring device based on the microfluidic system in this paper, there are several technical issues that require to be solved in the near future. 1) The glucose concentration of the sample in the collection chamber is lower than the glucose concentration of the ISF with a dilution factor around 10. A more sensitive glucose sensor than the common blood glucose sensor is needed. For this purpose, a high sensitive glucose sensor, which has long lifetime, based on surface plasmon resonance [22] is being studied in our group. This sensor will be integrated into the collection chamber. 2) For the current microfluidic system, the collection chamber has to be cleaned and dried up before next measurement. The interior surface of the collection chamber will be treated to obtain a hydrophobic surface for automatically expelling the sample from the collection chamber into a waste reservoir with vacuum pressure. 3) Experiments on human skin will be performed to find the appropriate parameters, such as the length of ultrasound pretreatment time and vacuum pressure, for ISF extraction through human skin and to evaluate the performance of the continuous glucose monitoring device.

V. CONCLUSION

This paper has demonstrated a microfluidic system for ISF extraction, collection, and volumetric measurement toward the application for glucose monitoring. A vacuum pressure of less than 91 kPa has been achieved from the vacuum generator in this system. A novel integrated flow sensor that is able to stably control the defined volume of normal saline injection and is capable of consistently measuring the volume of the extracted ISF has been demonstrated. This consistency is shown by the high correlation coefficient ($R^2 = 0.9992$) between the tested volume and the volume measured by a microsyringe in a simulated ISF extraction test. Under the management of the pneumatic valves and by using the 95-kPa vacuum force generated from the vacuum generator, this system has been proven to successfully extract "ISF analog" through ultrasound pretreated pig skin, manipulate fluid transport in the system, and accurately measure the volume of transdermally extracted ISF. The absolute error in the volume measurements of the transdermally extracted "ISF analog" is less than 0.05 μL. Future efforts will be concentrated on integrating a micro glucose sensor into the ISF collection chamber in the microfluidic system to form a complete continuous glucose monitoring device.

REFERENCES

[1] (2010). *Blood Glucose Meters*. [Online]. Available: http://www.diabetesnet.com/diabetes-technology/meters-monitors/blood-glucose-meters
[2] C. M. Girardin, C. Huot, M. Gonthier, and E. Delvin, "Continuous glucose monitoring: A review of biochemical perspectives and clinical use in type 1 diabetes," *Clin. Biochem.*, vol. 42, no. 3, pp. 136–142, Feb. 2009.
[3] S. Mitragotri, M. Coleman, J. Kost, and R. Langer, "Analysis of ultrasonically extracted interstitial fluid as a predictor of blood glucose levels," *J. Appl. Physiol.*, vol. 89, no. 3, pp. 961–966, Sep. 2000.
[4] R. G. Tiessen, M. M. Rhemrev-Boom, and J. Korf, "Glucose gradient differences in subcutaneous tissue of healthy volunteers assessed with ultraslow microdialysis and a nanolitre glucose sensor," *Life Sci.*, vol. 70, pp. 2457–2466, 2002.
[5] S. K. Garg, S. J. Fermi, R. O. Potts, J. A. Tamada, N. R. Ackerman, and H. P. Chase, "Correlation of fingerstick blood glucose measurements with GlucoWatch biographer glucose results in young subjects with type 1 diabetes," *Diabetes Care*, vol. 22, no. 10, pp. 1708–1714, Oct. 1999.
[6] S. Gebhart, M. Faupel, R. Fowler, C. Kapsner, D. Lincoln, V. McGee, J. Pasqua, L. Steed, M. Wangsness, F. Xu, and M. Vanstory, "Glucose sensing in transdermal body fluid collected under continuous vacuum pressure via micropores in the stratum corneum," *Diabetes Technol. Therapeutics*, vol. 5, no. 2, pp. 159–166, Jul. 2004.
[7] S. Zimmermann, D. Fienbork, B. Stoeber, A. W. Flounders, and D. Liepmann, "A microneedle-based glucose monitor: Fabricated on a wafer-level using in-device enzyme immobilization," in *Proc. Transducers*, 2003, pp. 99–102.

[8] A. Tura, A. Maran, and G. Pacini, "Non-invasive glucose monitoring: Assessment of technologies and devices according to quantitative criteria," *Diabetes Res. Clin. Pract.*, vol. 77, no. 1, pp. 16–40, Jul. 2007.
[9] A. Sieg, R. H. Guy, and M. B. Delgado-Charro, "Noninvasive and minimally invasive methods for transdermal glucose monitoring," *Diabetes Technol. Therapeutics*, vol. 7, no. 7, pp. 174–197, 2005.
[10] T. Bailey, H. Zisser, and A. Chang, "New features and performance of a next-generation seven-day continuous glucose monitoring system with short lag time," *Diabetes Technol. Therapeutics*, vol. 11, no. 12, pp. 749–755, Dec. 2009.
[11] J. Mastrototaro, J. Shin, A. Marcus, and G. Sulur, "The accuracy and efficacy of real-time continuous glucose monitoring sensor in patients with type 1 diabetes," *Diabetes Technol. Therapeutics*, vol. 10, no. 5, pp. 385–390, Oct. 2008.
[12] R. L. Weinstein, S. L. Schwartz, R. L. Brazg, J. R. Bugler, T. A. Peyser, and G. V. McGarraugh, "Accuracy of the 5-day FreeStyle navigator continuous glucose monitoring system," *Diabetes Care*, vol. 30, no. 5, pp. 1125–1130, May 2007.
[13] J. C. Pickup, F. Hussain, N. D. Evans, and N. Sachedina, "In vivo glucose monitoring: The clinical reality and the promise," *Biosens. Bioelectron.*, vol. 20, no. 10, pp. 1897–1902, Apr. 2005.
[14] J. Kost, S. Mitragotri, R. A. Gabbay, M. Pishko, and R. Langer, "Transdermal monitoring of glucose and other analytes using ultrasound," *Nat. Med.*, vol. 6, no. 3, pp. 347–350, Mar. 2000.
[15] A. Nanda, S. Nanda, and N. M. K. Ghilzai, "Current developments using emerging transdermal technologies in physical enhancement methods," *Current Drug Del.*, vol. 3, no. 3, pp. 233–242, Jul. 2006.
[16] H. Benson, "Transdermal drug delivery: Penetration enhancement techniques," *Current Drug Del.*, vol. 2, no. 1, pp. 23–33, Jan. 2005.
[17] S. K. Li, A. Ghanem, K. D. Peck, and W. I. Higuchi, "Characterization of the transport pathways induced during low to moderate voltage iontophoresis in human epidermal membrane," *J. Pharm. Sci.*, vol. 87, no. 1, pp. 40–48, Jan. 1998.
[18] S. Mitragotri, D. Blankschtein, and R. Langer, "Transdermal drug delivery using low-frequency sonophoresis," *Pharm. Res.*, vol. 13, no. 3, pp. 411–420, Mar. 1996.
[19] J. Gupta and M. R. Prausnitz, "Recovery of skin barrier properties after sonication in human subjects," *Ultrasound Med. Biol.*, vol. 35, no. 8, pp. 1405–1408, Aug. 2009.
[20] H. Yu, J. Liu, T. Shi, D. Li, Z. Du, and K. Xu, "Using skin impedance to improve prediction accuracy of continuous glucose monitoring system," in *Proc. SPIE*, 2008, p. 686 30S.
[21] X. Niu, S. Peng, L. Liu, W. Wen, and P. Sheng, "Characterizing and patterning of PDMS-based conducting composites," *Adv. Mater.*, vol. 19, no. 18, pp. 2682–2686, Sep. 2007.
[22] F. Huang, D. Li, B. Song, P. Wu, J. Zhang, and K. Xu, "Measurement of glucose concentration by surface plasmon resonance with D-galactose/D-glucose binding protein," *Nanotechnol. Precision Eng.*, vol. 8, pp. 132–136, 2010.

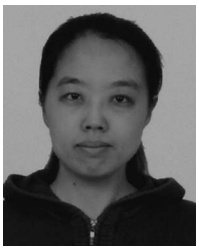

Haixia Yu received the Ph.D. degree in precision instrument and optoelectronics engineering from Tianjin University, Tianjin, China, in 2011.

From 2008 to 2010, she studied in the Department of Electrical Engineering and Computer Science, Case Western Reserve University, USA, as a joint Ph.D. student. Presently, she is conducting postdoctoral research on an interstitial fluid transdermal extraction system based on microfluidics.

Dachao Li received the Ph.D. degree in precision instrument and optoelectronics engineering from Tianjin University, Tianjin, China, in 2004.

From 2004 to 2006, he conducted postdoctoral research at Peking University, China. From 2006 to 2008, he was a Research Associate in the Department of Electrical Engineering and Computer Science, Case Western Reserve University, Cleveland, OH. Presently, he is an Associate Professor in the College of Precision Instrument and Optoelectronics Engineering, Tianjin University. His research specialization is biomedical micro sensors and micro instruments.

Robert C. Roberts received the B.S. and M.S. degrees in systems and control engineering from Case Western Reserve University (CWRU), Cleveland, OH, in 2005 and 2006, respectively, where he is currently working toward the Ph.D. degree in electrical engineering with a focus on microelectromechanical systems (MEMS).

His M.S. research focused on the development of software-defined radio. From 2005 to 2006, he served as a Laboratory Technician in the John G. Breen Technology Center at Sherwin-Williams Company, Cleveland, OH. Since 2006, he has served as a Research Assistant at CWRU. His research interests focus on novel MEMS-based technologies using inkjet printing.

Kexin Xu received the Ph.D. degree in precision instrument and optoelectronics engineering from Tianjin University, Tianjin, China, in 1988.

He is currently a Professor in the College of Precision Instrument and Optoelectronics Engineering, Tianjin University. His current research interests include bio-optical measurement and spectroscopy technology.

Norman C. Tien received the Ph.D. degree in electrical engineering from the University of California at San Diego, La Jolla.

He was a Faculty Member in the Department of Electrical and Computer Engineering, Cornell University, Ithaca, NY, from 1997 to 2002. He also served as Chair of the Department of Electrical and Computer Engineering, University of California, Davis, and held a joint appointment at the University of California, Berkeley. He is currently the Dean and Nord Professor of Engineering at Case Western Reserve University, Cleveland, OH. He is also the Ohio Eminent Scholar in Condensed Matter Physics. His research interests include the fabrication of small structures, tools, and instruments for use in wireless communications, biomedical systems, and environmental monitoring.